Supplementary Data

Luminescence dating procedures and protocols

Sample preparation

Samples were prepared and analyzed at the Desert Research Institute Luminescence Laboratory (DRILL) using standard procedures (Aitken, 1998). Samples were sieved to the coarsest available fine sand fraction; in most cases this included either the 125-180 µm fraction or the 180-250 µm fraction. Wider particle size ranges (125-250 µm) were used for samples with limited material available for measurement. Samples were deflocculated using sodium pyrophosphate decahydrate ($Na_4P_2O_7.10H_2O$), wet sieved, then treated with 10% HCl acid and 30% H_2O_2 solution to remove carbonates and organics, respectively. The magnetic sub-fraction was then removed using a hand magnet and mineral density separation was conducted using heavy liquid lithium heteropolytungstate to isolate quartz grains at $2.62 < \rho < 2.68$ gcm^{-3}. Quartz grains were treated with 48% hydrofluoric acid (HF) to remove the outer alpha-irradiating rind of the grains; this simplifies dose rate calculations. Treatment included a 60 min HF etch followed by a 10% HCl acid treatment for ~10 hours. These samples were then sieved to remove grains that were reduced to below the lower grain size limit by the HF etch. Initial measurements on single grains of quartz from sample Qt2-1 yielded poor results (i.e., <5% of grains had a natural signal brighter than the background signal). Therefore, all subsequent measurements were made on multi-grain aliquots, where quartz grains were mounted on 10 mm diameter stainless steel discs using silicone oil as an adhesive.

Preheat plateau and dose recovery tests

Preheat plateau and dose recovery tests were conducted on sample Qt2-1 (180-250 µm fraction) to determine the optimal single-aliquot regenerative dose (SAR) measurement parameters for equivalent dose (D_e) measurement in this study. The preheat plateau test was conducted on 4 mm diameter multi-grain aliquots (~220 grains per aliquot) that were bleached in a Risø reader twice for 1000 s at 125 °C to deplete their signal and subsequently given a laboratory beta dose of 23 Gy. The sample was then measured using a SAR protocol with preheats (step 2 in Table S1) that ranged from 160 °C to 300 °C, and a cutheat of 160 °C. A hotwash was also included in the SAR protocol that was 20 °C higher than each preheat tested, as employing a hotwash that is close to, or higher than the preheat has been shown to reduce recuperation in quartz (Murray and Wintle, 2003; Murray et al., 2021). Our preheat plateau test result shows that preheats of 160-220 °C provide the most optimal results where the measured/given dose

ratio (average of 3 aliquots for each preheat) lies within 10% of unity, recuperation is less than 5% of the natural signal, and recycling ratios are within 10% of unity (Fig. S1).

Our results also showed that 4 mm diameter aliquots yield test dose luminescence signals (Tn) that are bright (>3000 counts per second), suggesting that we could afford to measure this sample using smaller aliquots (fewer grains per aliquot) to increase the resolution of our D_e distributions and reduce signal averaging effects from multiple grains. Single-grain measurements (above) showed that less than 5% of grains from sample Qt2-1 yielded a natural signal greater than the background signal, so we expect that, for 2 mm diameter aliquots (55-110 grains), less than 10 grains per aliquot will luminescence, further reducing grain signal averaging effects.

A dose recovery test was subsequently performed on sample Qt2-1 using a preheat of 180 °C (10 s), a cutheat of 160 °C and a hotwash measured at 200 °C (Table S1). This test was conducted on smaller 2 mm diameter multi-grain aliquots (~55-110 grains) to increase the resolution of our D_e distribution. Out of 48 measured aliquots, 29 passed all aliquot rejection criteria (Fig. S1) and no aliquots were rejected due to dim test dose (Tn) signals (i.e., less than 3 times the background signal) or test dose signals with greater than 10% error. The resulting weighted mean measured-to-given dose ratio (calculated using the Central Age Model of Galbraith et al. (1999)) was 1.02 ± 0.02 with an overdispersion of 7 ± 2%. Therefore, we concluded that our chosen SAR protocol and aliquot size are appropriate for these samples.

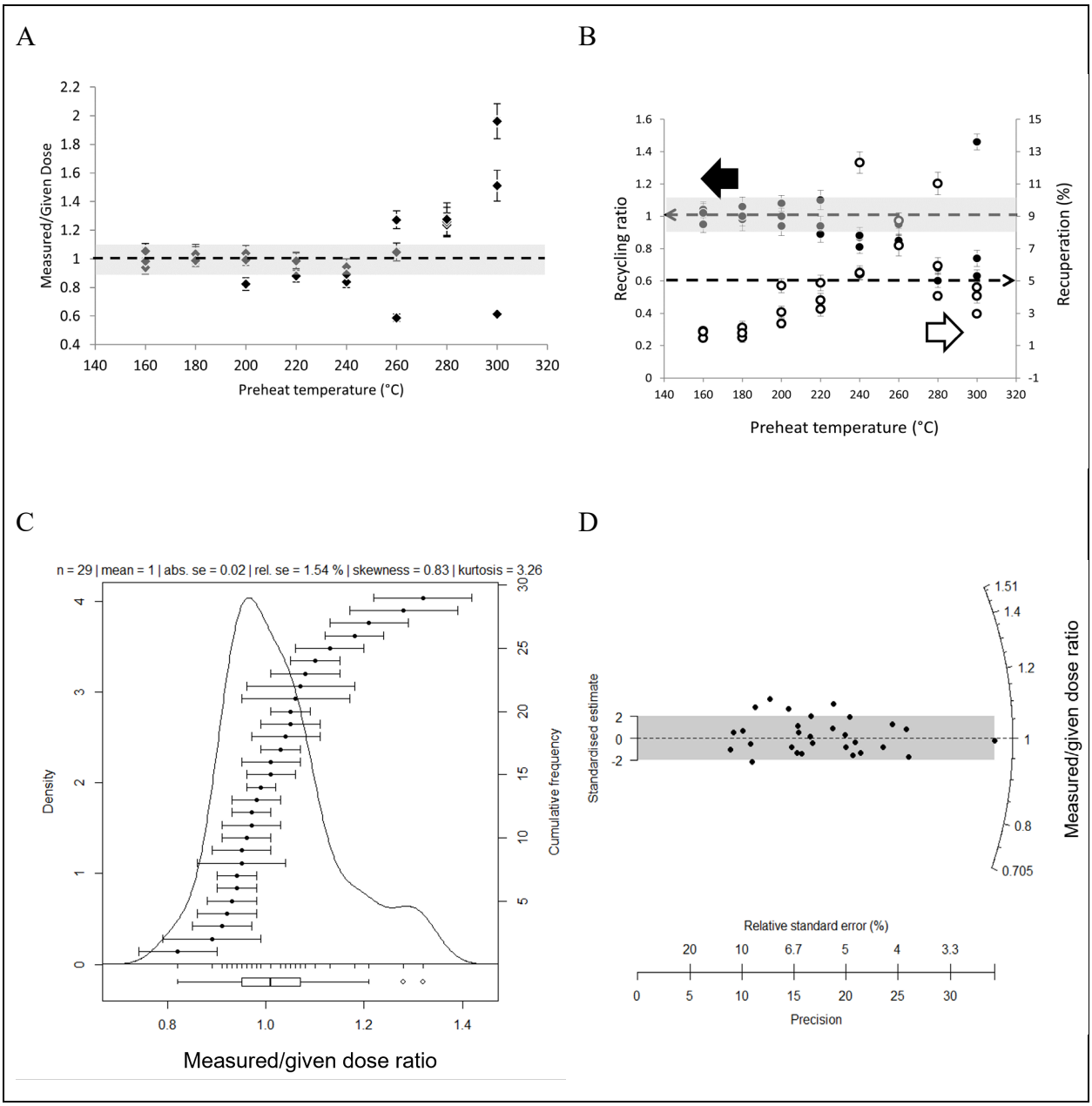

Figure S1. Preheat plateau and dose recovery test results for sample Qt2-1. A) Preheat plateau measured/given dose ratios for each tested preheat ranging from 160 °C to 300 °C. Three multi-grain aliquots were measured for each preheat. Points that lie in the grey shaded region are within 10% of unity. B) Recycling ratio (solid circles) and recuperation values (open circles) for each measured aliquot shown in 'A'. Recycling ratios that lie in the grey shaded region are within 10% of unity. C) The measured/given dose ratios for all 29 accepted aliquots measured during the dose recovery test plotted as points in ascending order superimposed on a cumulative Kernel Density Estimate curve. D) The measured/given dose ratios for the dose recovery test in

C) plotted in a radial plot. Points that fall within the grey shaded region are within 2 sigma of a measured/given dose ratio of 1.0.

Equivalent dose determination

The equivalent dose (D_e) of multi-grain aliquots from all samples was measured using the single aliquot regenerative-dose (SAR) technique (Murray and Wintle 2000, 2003) using the parameters outlined in Table S1 as determined from preheat plateau and dose recovery tests above. Steps 1-7 of the protocol constitute one SAR cycle. The first SAR cycle measures the sensitivity corrected natural signal, and subsequent SAR cycles measure the regenerative-dose signals (Lx/Tx) after a series of successively increasing laboratory radiation doses administered to the sample. The regeneration doses are used to generate a dose-response curve (i.e., Lx/Tx vs regenerative dose) onto which the natural signal (Ln/Tn) is plotted to calculate the D_e value. Regeneration doses include one "zero-dose" point where no radiation dose is given to measure recuperation of signal, and one "repeat-dose" point, where a previous regeneration dose is measured a second time to calculate the recycling ratio. See Murray and Wintle (2000) and Murray and Wintle (2003) for details.

Table S1. The SAR dating protocol used in this study[*i]

Step	Sample treatment
1	Natural/Regenerative Dose
2	Preheat (180°C, 10 s)
3	Blue LED stimulation (125°C, 100 s) → L_n, L_x
4	Test dose (~4 Gy)
5	Cutheat (160°C, 0 s)
6	Blue LED stimulation (125°C, 100 s) → T_n, T_x
7	Blue LED stimulation (200°C, 40 s)
8	Return to step 1.

[*]Ln = natural signal, Lx = regenerative dose signal. Tn = test dose signal measured after Ln, Tx = test dose signal measured after Lx. LED stands for light emitting diodes.

Dose response curves were fitted with an exponential plus linear curve. Routine screening criteria included rejection of aliquots that exhibited the following behavior:

- Poor signals as judged from net natural test dose (Tn) signals that are less than three times the standard deviation of the background signal.
- Failure to reproduce, to within 10%, the same sensitivity-corrected luminescence signal from identical regeneration doses given at the beginning and end of the SAR sequence, which suggests inaccurate sensitivity correction (recycling test).

- Failure to reproduce, to within 10%, a sensitivity-corrected regenerative dose signal after stimulation with IR light (i.e., the IR depletion ratio test for feldspar contamination).
- A test dose error of >10%.
- Recuperation (i.e., the Lx/Tx value measured after the "zero-dose" point regenerative dose) that is > 5% of the sensitivity-corrected natural signal (Ln/Tn).

Dose rate and age calculations

Samples for dose rate were dried and milled to a fine, flour consistency and sent to ALS Geochemistry in Reno, NV for geochemical analysis of U, Th, Rb and K_2O. Subsamples used for U, Rb and Th measurement were fused with lithium borate and measured with ICP-MS. K_2O was measured on bulk sample with ICP-AES and converted to % K. Dose rates (Gy/ka) were calculated using the conversion factors of Liritzis *et al.* (2013) and are shown to 2 decimal places (Table S2); ages were calculated prior to rounding. Measured water contents ranging from ~1 to 11% (expressed as the percentage of the mass of dry sediment) were used for age calculations. These values were used to represent the water content of the sediments for their lifetime of burial. Cosmic dose rates (Gy/ka) were calculated according to Prescott and Hutton (1994) (Table S2). Dose rate and final age calculations were made using DRAC (Durcan *et al.* 2015). Ages are expressed as thousands of years before A.D. 2018 and rounded to the nearest 10 years (Table 2).

The youngest/modern samples with dim signals had the highest number of rejected aliquots. Aliquots were rejected mainly due to poor photon statistics or recuperation of signal that was higher than 5% of the natural signal. For instance, for samples Qt7 (1) and Qt7 (2), only 16 and 10 aliquots, respectively, passed all rejection criteria out of 120 measured aliquots for each sample (Table 2). Therefore, these ages must be interpreted with caution.

Kernel density estimates (KDE) and radial plots (Fig. S1) were used to examine the distribution of D_e values to infer possible sources of scatter and to check for elevated positive skewness that may be indicative of incomplete bleaching of grains in a fluvial environment (cf. Rittenour, 2008) (Fig. S2). All samples except for the youngest ancient sample (Qt5 (1)) and the two modern surface samples (Qt7 (1) and Qt7 (2)) had overdispersion (OD) values of 29% or less (Table 2) and near-symmetrical D_e distributions, suggestive of near-complete sun exposure of grains prior to burial. These OD values are within the range of those reported for samples known, or thought, to have been fully bleached at the time of deposition by Arnold and Roberts (2009, Table 5). The KDE plots of samples Qt2-1, Qt4-3, Qt3 (1) and Qf1/Qt1 each show a secondary hump, which may be attributed to some mixing between sedimentary layers due to bioturbation/pedogenesis, heterogeneities in the dose rate field at the sample site, aliquot-to-

aliquot variations in optical properties, and/or measurement error (Aitken, 1998). Unfortunately, our data do not allow us to differentiate between these sources of scatter with confidence, nor to determine which hump more accurately approximates the true sample age. Given the low OD values for these samples, and their near-symmetrical D_e distributions, the sample equivalent (or burial) dose (D_b) was modeled using the Central Age Model (CAM) of Galbraith et al. (1999), which assumes complete bleaching of all grains (Fig. S2).

The youngest ancient sample, Qt5 (1), and modern samples Qt7 (1) and Qt7 (2) yielded high OD values (90%, 101% and 111%, respectively) and highly skewed D_e distributions suggestive of incomplete bleaching (Table 2, Fig. S2). Because these samples are very young to modern, it is expected that their D_e distributions will be more sensitive to partial bleaching effects as residual doses will constitute a larger proportion of their paleodose (Madsen and Murray, 2009). The D_b values for these samples were calculated using the Minimum Age Model (MAM) of Galbraith et al. (1999), which targets the most recently bleached grains in a partially bleach D_e distribution (Fig. S2).

Environmental dose rate data

Table S2. Dose rate data for luminescence samples in this study.

Sample	Depth (m)	Grain size fraction[1] (μm)	U (ppm)	Th (ppm)	Rb (ppm)	K (%)	External beta dose rate (Gy/ka)	External gamma dose rate (Gy/ka)	Cosmic dose rate (Gy/ka)	Total dose rate (Gy/ka)
Qt7 (1)	0.03	125-250	2.74	10.10	79.9	0.87	1.17 ± 0.13	0.71 ± 0.06	0.33 ± 0.03	2.20 ± 0.14
Qt7 (2)	0.03	125-180	2.63	10.30	72.3	0.90	1.11 ± 0.12	0.66 ± 0.05	0.33 ± 0.03	2.10 ± 0.14
Qt5 (1)	2.05	185-250	2.29	7.95	71.7	1.69	1.68 ± 0.13	1.05 ± 0.06	0.19 ± 0.02	2.91 ± 0.14
Qt5 (2)	1.35	180-250	3.00	8.90	73.7	0.82	1.15 ± 0.13	0.95 ± 0.07	0.20 ± 0.02	2.30 ± 0.15
Qt4-3	3.60	125-180	3.08	9.49	76.8	1.77	1.91 ± 0.14	1.22 ± 0.07	0.16 ± 0.02	3.29 ± 0.16
Qt3 (2)	2.10	185-250	3.02	9.37	63.8	1.78	1.86 ± 0.14	1.22 ± 0.07	0.19 ± 0.02	3.26 ± 0.16
Qt3 (1)	2.10	180-250	3.11	12.60	63.6	0.85	1.26 ± 0.13	1.15 ± 0.08	0.19 ± 0.02	2.59 ± 0.15
Qt2-1	1.70	185-250	2.61	8.06	57.2	1.49	1.56 ± 0.11	1.03 ± 0.06	0.20 ± 0.02	2.78 ± 0.13
Qt2-2	0.80	180-250	2.03	6.22	49.8	0.79	0.96 ± 0.13	0.72 ± 0.07	0.22 ± 0.02	1.89 ± 0.15
Qf1/Qt1	4.50	125-180	3.00	8.87	62.6	0.93	1.26 ± 0.13	0.97 ± 0.08	0.14 ± 0.01	2.37 ± 0.16

[1]Samples were sieved to the coarsest available fine sand fraction. Wider particle size ranges were used for samples with limited material available for measurement.

Qt5 (1)

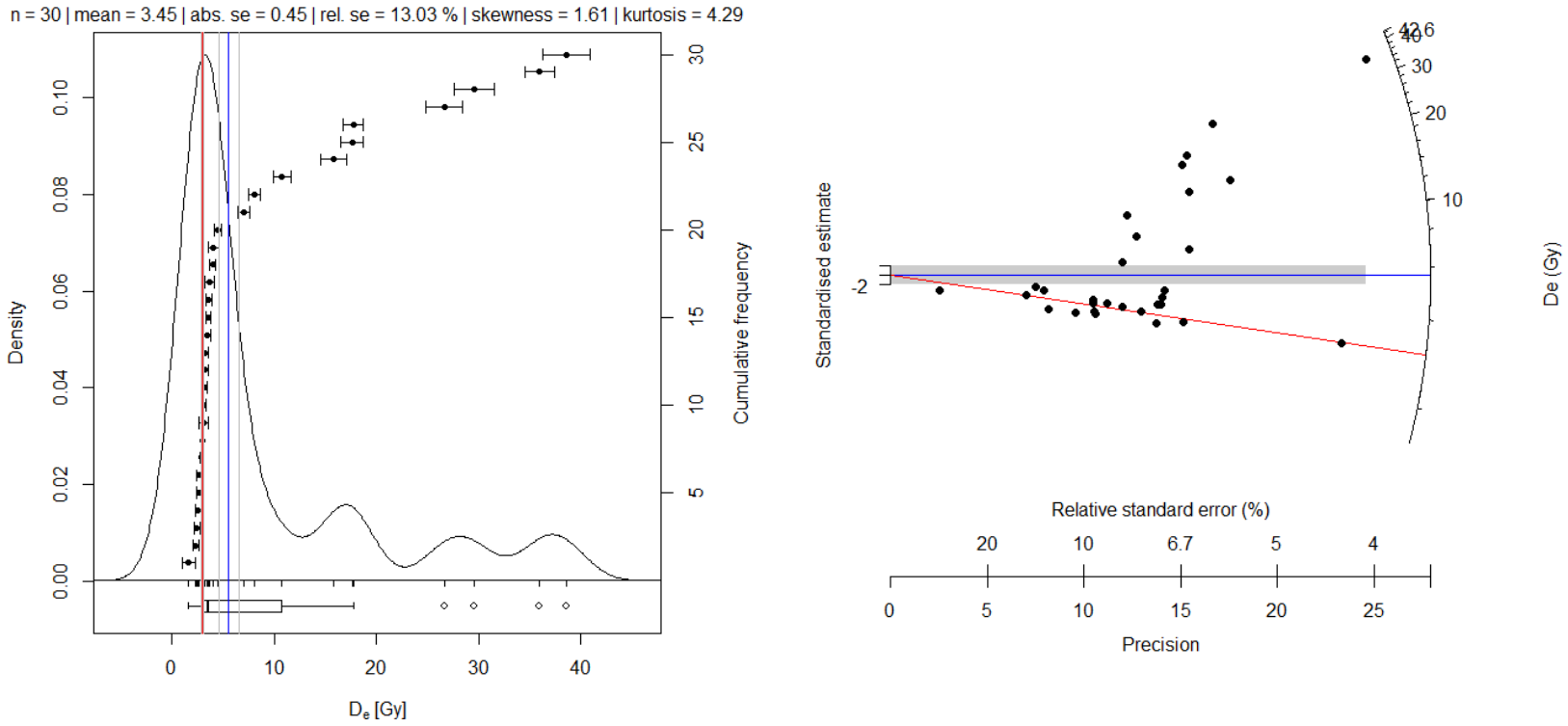

Figure S2. *De* distributions for all samples. Kernel density estimates (KDE) (left) and radial plots (right) were generated using the Luminescence Package for R (Kreutzer *et al.* 2020). Blue lines are centered on the CAM weighted mean *De* value, and red lines are centered on the MAM *De* value, where calculated. Grey lines shown in the KDE plots mark the ±1 sigma errors of the CAM and MAM *De* values. All radial plots are centered on the CAM weighted mean *De* value, and points that lie within the shaded region are within 2 standard deviations of the CAM weighted mean.

Qt3 (2)

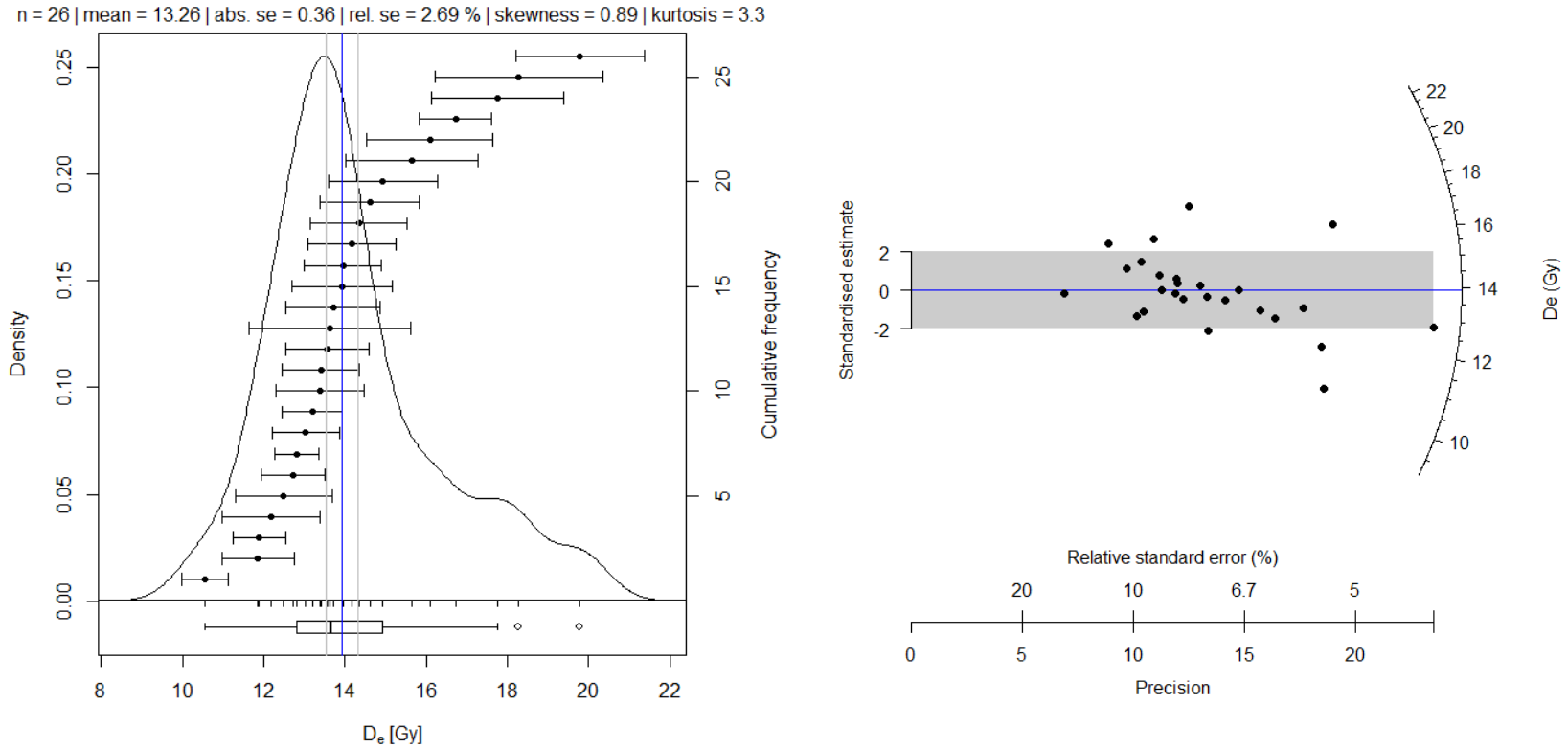

Figure S2, continued.

Qt2-1

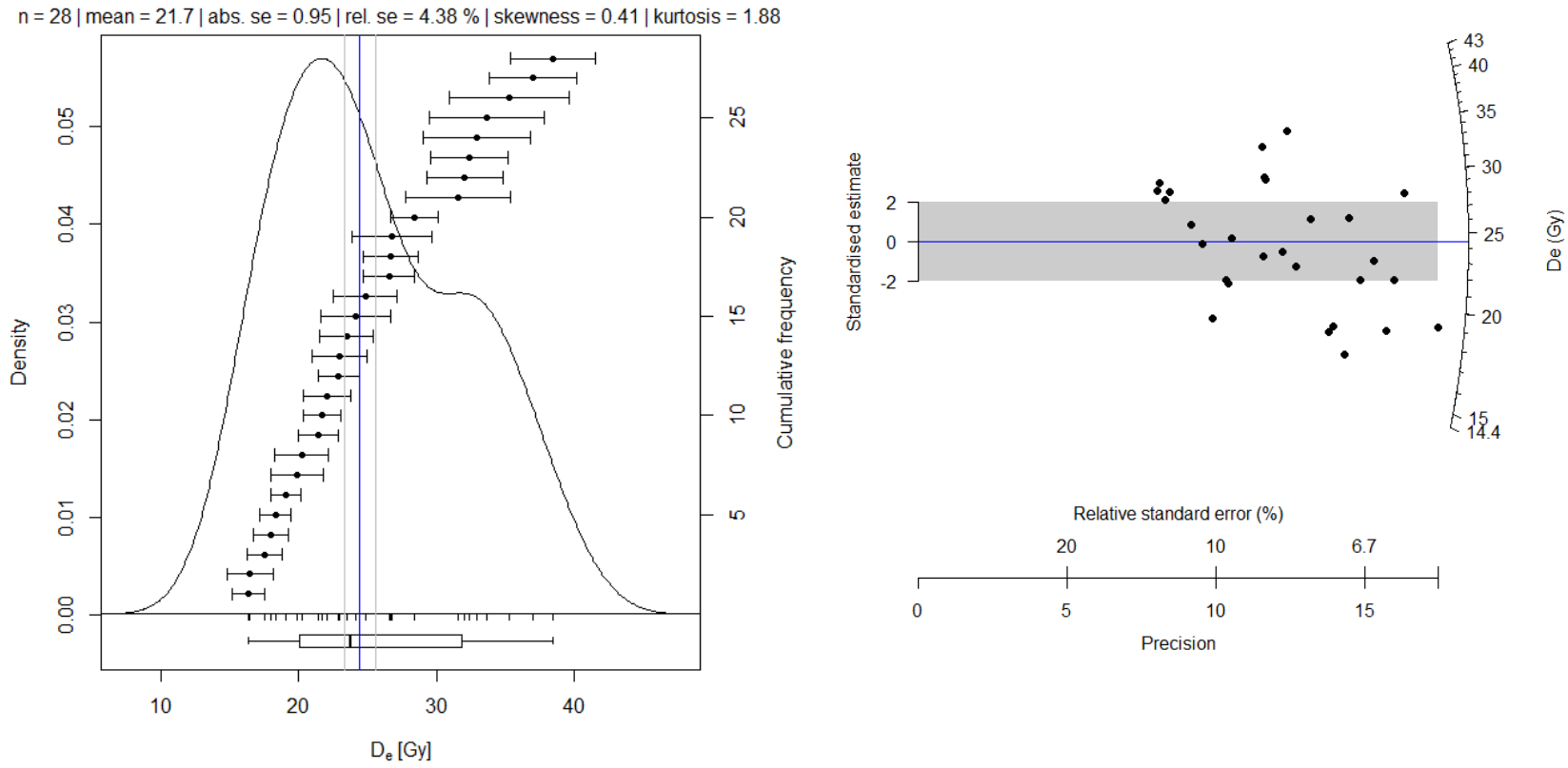

Figure S2, continued.

Qt4-3

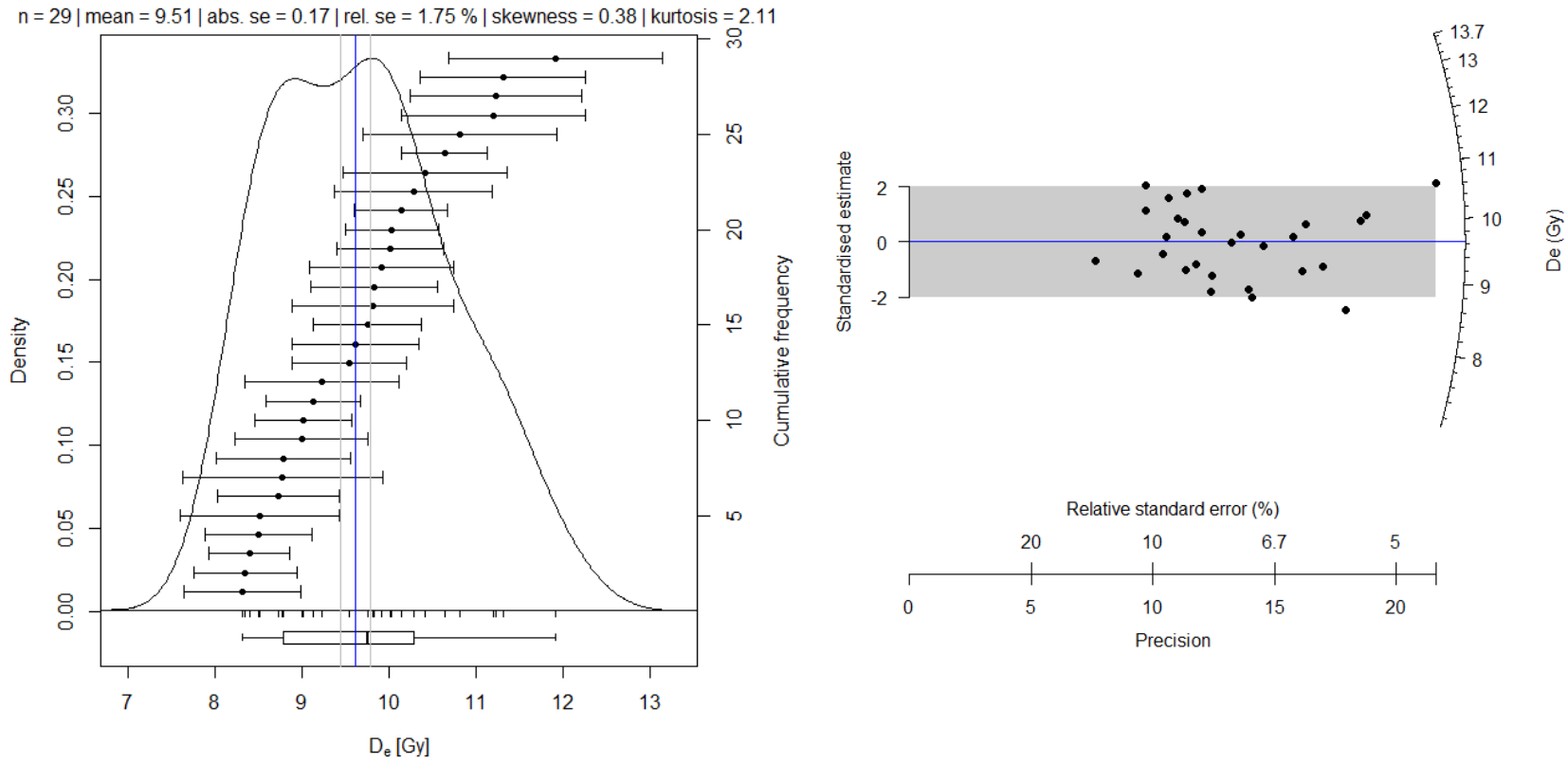

Figure S2, continued.

Qt2-2

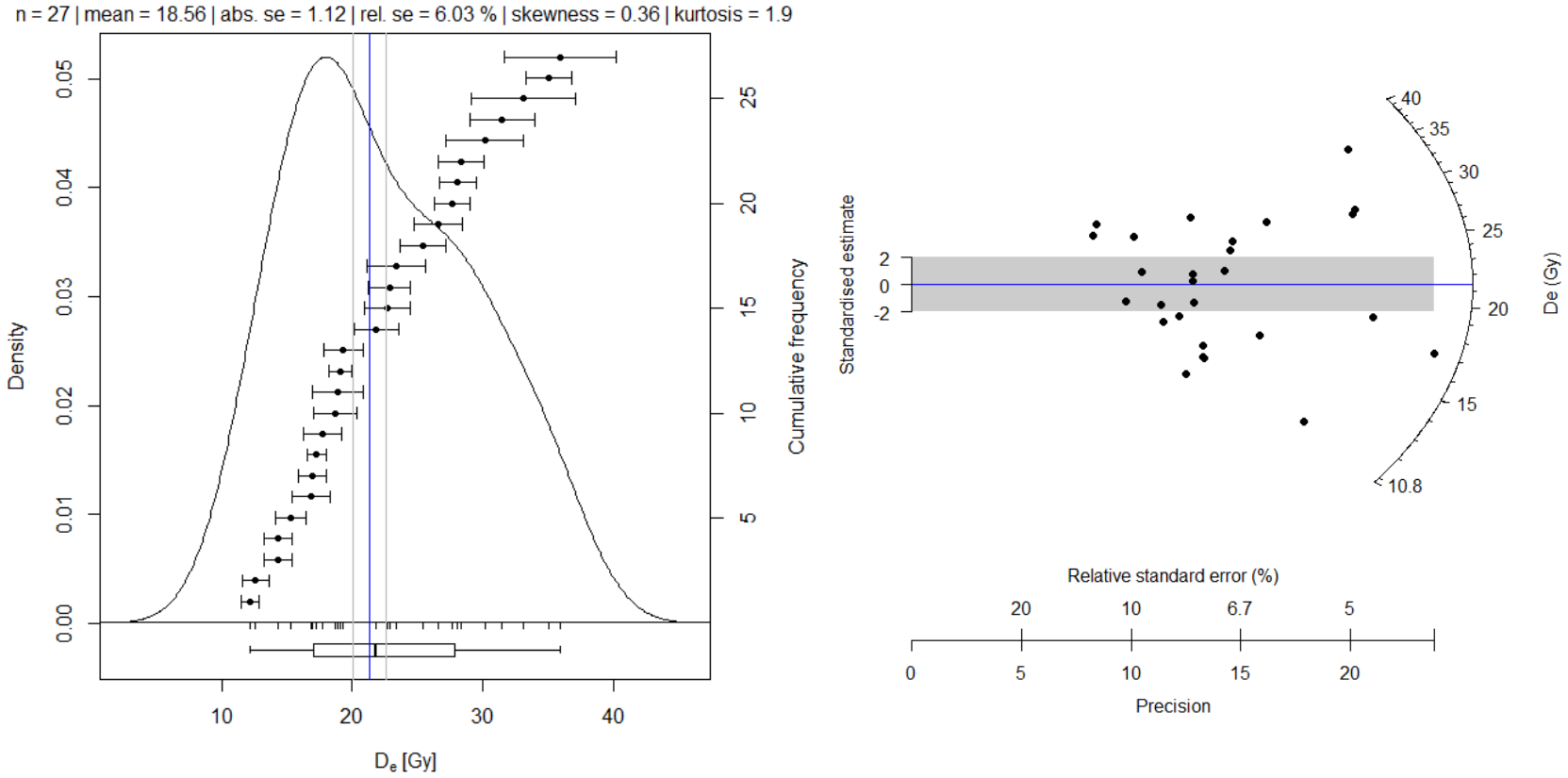

Figure S2, continued.

Qt5 (2)

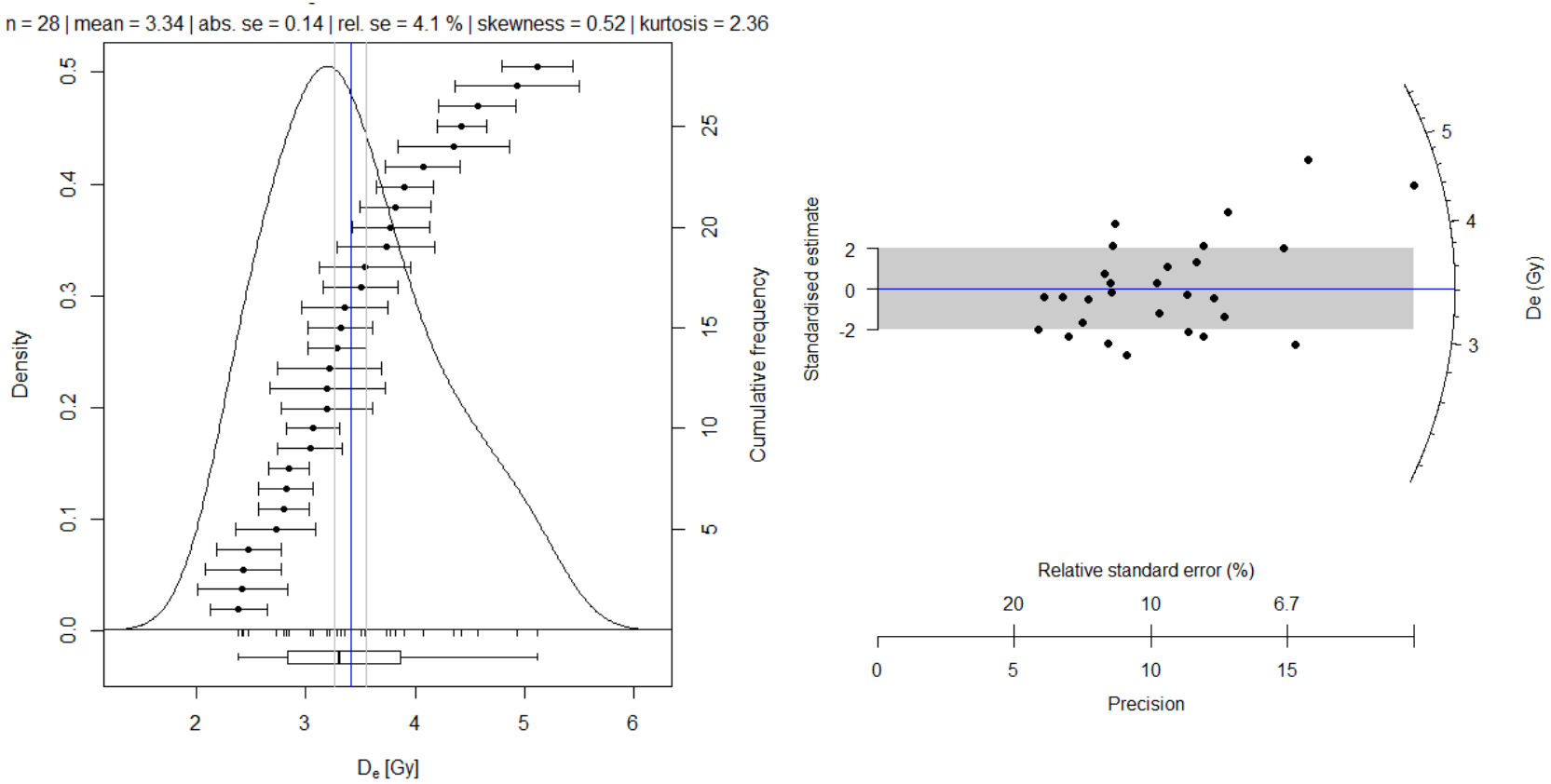

Figure S2, continued.

Qt3 (1)

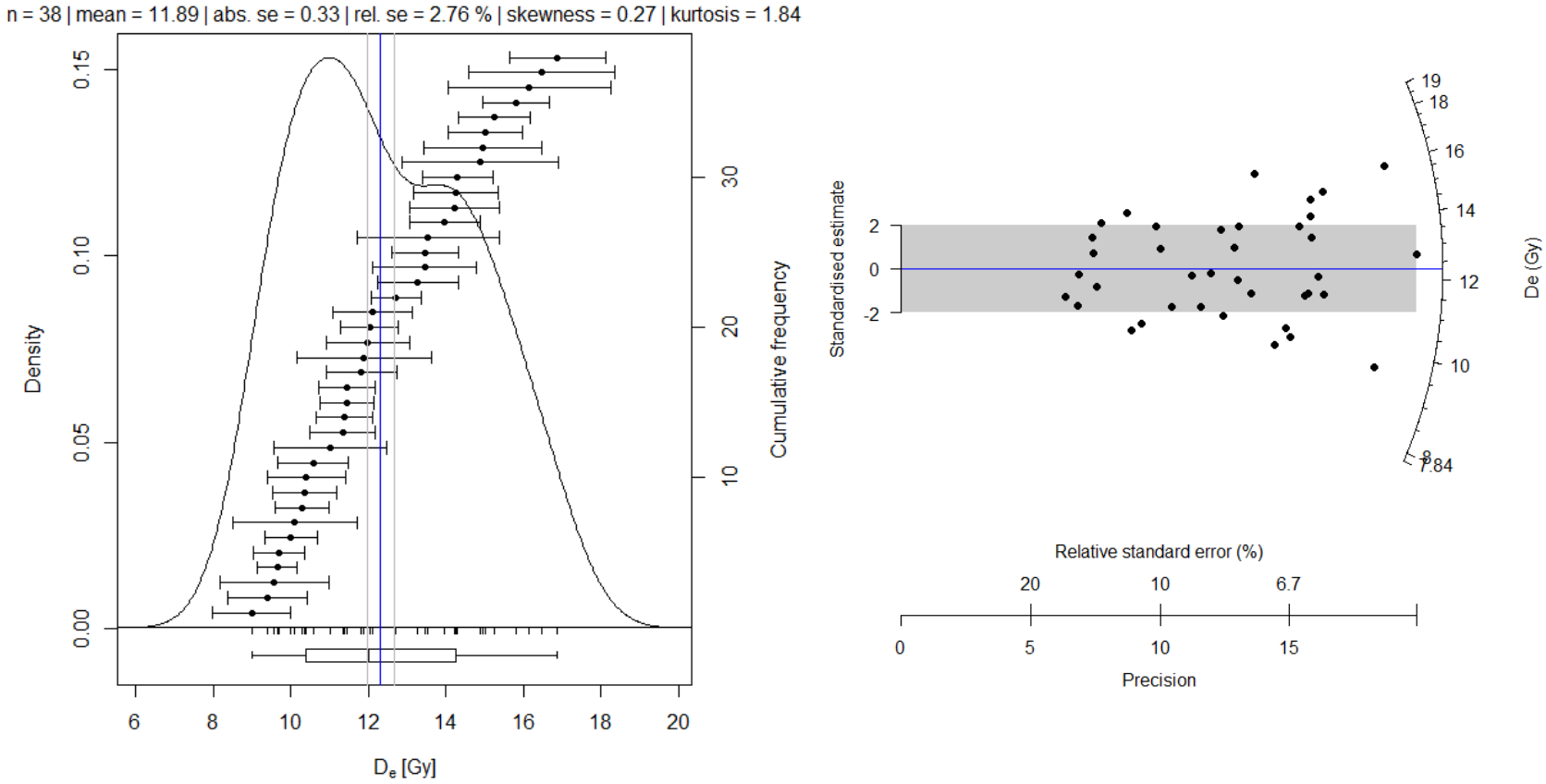

Figure S2, continued.

Qt7 (1)

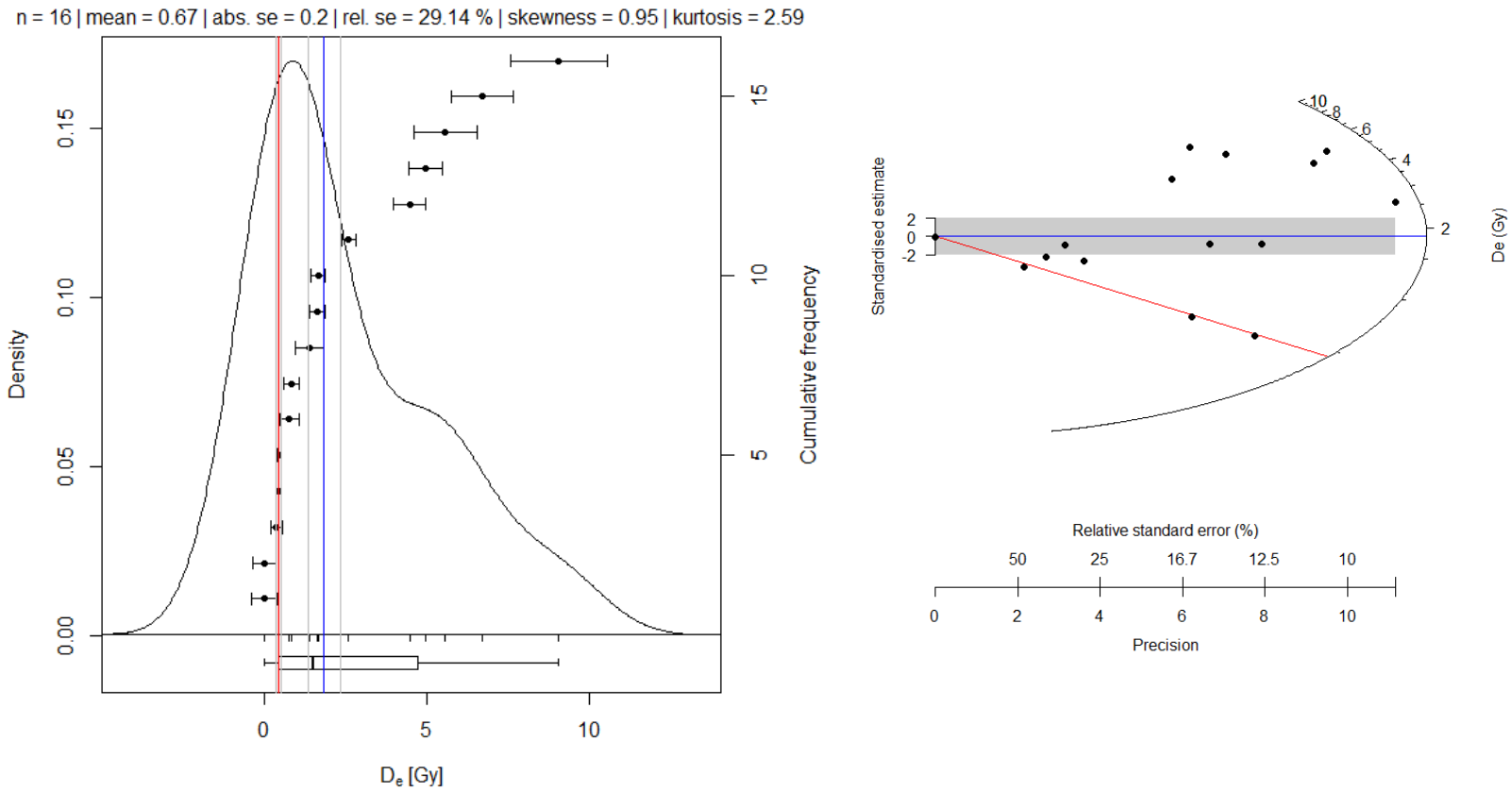

Figure S2, continued.

Qt7 (2)

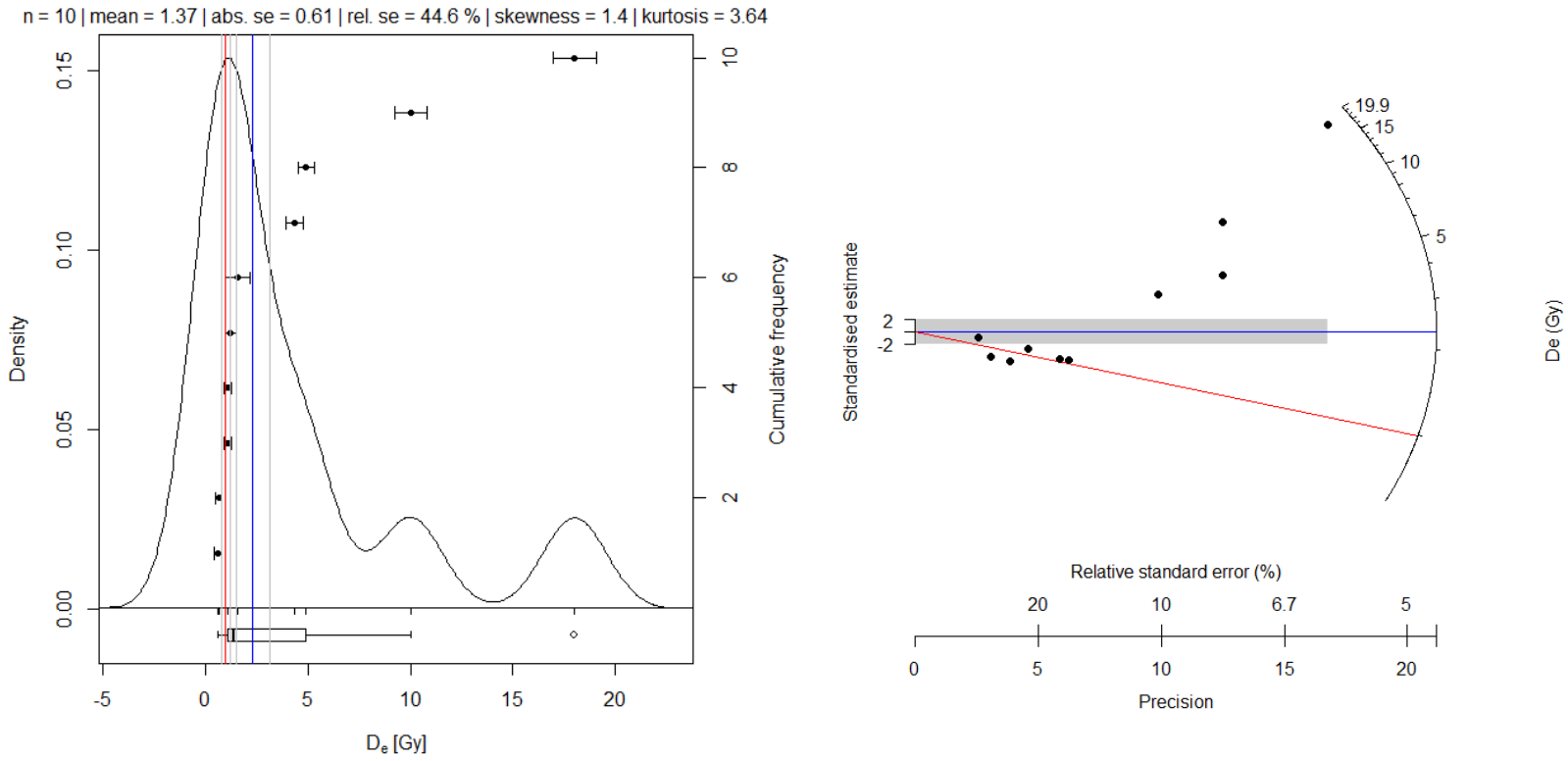

Figure S2, continued.

Qf1/Qt1

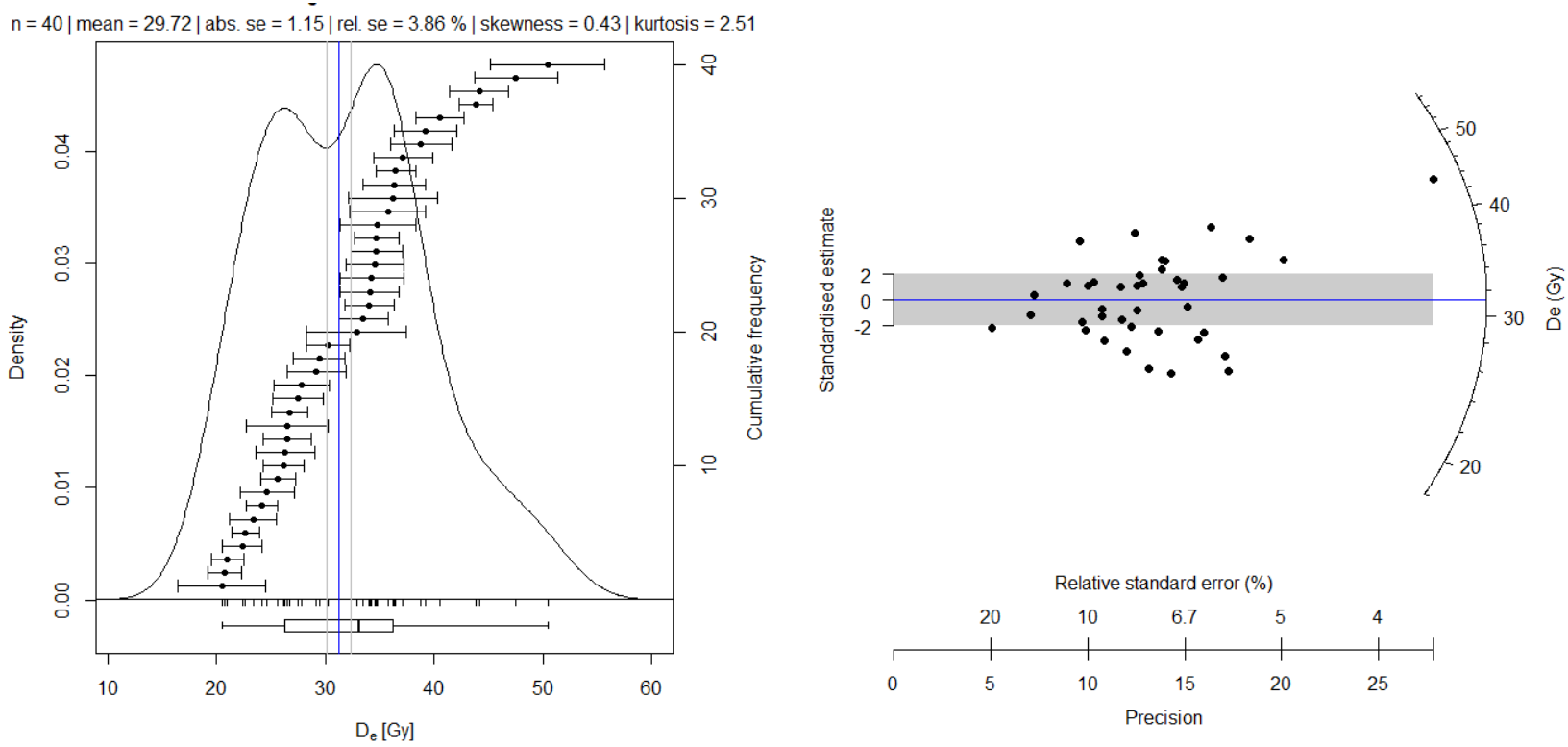

Figure S2, continued.

References

Aitken, M.J. 1998. An Introduction to Optical Dating: The Dating of Quaternary Sediments by the Use of Photon-Stimulated Luminescence. Oxford University Press. 267 pp.

Arnold, L.J. and Roberts, R.G. 2009. Stochastic modelling of multi-grain equivalent dose (De) distributions: Implications for OSL dating of sediment mixtures. Quaternary Geochronology, 4, 204-230, https://doi:10.1016/j.quageo.2008.12.001.

Durcan, J.A., King, G.E. and Duller, G.A.T. 2015. DRAC: Dose Rate and Age Calculator for trapped charge dating. Quaternary Geochronology, 28, 54-61, https://doi.org/10.1016/j.quageo.2015.03.012.

Galbraith, R.F., Roberts, R.G., Laslett, G.M., Yoshida, H. and Olley, J.M. 1999. Optical dating of single and multiple grains of quartz from Jinmium Rock Shelter, northern Australia: Part I, Experimental design and statistical models. Archaeometry, 41, 339-364, https://doi.org/10.1111/j.1475-4754.1999.tb00987.x.

Kreutzer, S., Burow, C., Dietze, M., Fuchs, M.C., Schmidt, C., Fischer, M. and Friedrich, J. 2020. Luminescence: Comprehensive Luminescence Dating Data Analysis R package version 0.9.7, https://CRAN.R-project.org/package=Luminescence.

Liritzis, I., Singhvi, A.K., Feathers, J.K., Wagner, G.A., Kadereit, A., Zacharias, N. and Li, S.-H. 2013. Luminescence dating in archaeology, anthropology, and geoarchaeology: an overview. Springer.

Murray, A.S., Arnold, L.J., Buylaert, J.- P., Guérin, G., Qin, J., Singhvi, A.K., Smedley, R. and Thomsen, K. 2021. Optically stimulated luminescence dating using quartz. Nature Reviews Methods Primers 1, 72, https://doi.org/10.1038/s43586-021-00068-5.

Murray, A.S. and Wintle, A.G. 2000. Luminescence dating of quartz using an improved single-aliquot regenerative-dose protocol. Radiation Measurements, 32, 57-73, https://doi.org/10.1016/S1350-4487(99)00253-X.

Murray, A.S. and Wintle, A.G. 2003. The single aliquot regenerative dose protocol: potential for improvements in reliability. Radiation Measurements, 37, 377-381, https://doi.org/10.1016/S1350-4487(03)00053-2.

Prescott, J.R. and Hutton, J.T. 1994. Cosmic ray contributions to dose rates for luminescence and ESR dating: Large depths and long-term time variations. Radiation Measurements, 23, 497-500, https://doi.org/10.1016/1350-4487(94)90086-8.

Rittenour, T., 2008. Luminescence dating of fluvial deposits: applications to geomorphic, palaeoseismic and archaeological research. Boreas, 37, 613-635, https://doi.org/10.1111/j.1502-3885.2008.00056.x.